



# Gelation of $\beta$ -lactoglobulin in the presence of propylene glycol alginate: kinetics and gel properties

R. Baeza<sup>a,1</sup>, Luis M. Gugliotta<sup>b,1</sup>, A.M.R. Pilosof<sup>a,1,\*</sup>

<sup>a</sup> *Departamento de Industrias, Facultad de Ciencias Exactas y Naturales, Universidad de Buenos Aires, Ciudad Universitaria Nunez, Buenos Aires 1428, Argentina*

<sup>b</sup> *INTEC (Universidad Nacional del Litoral, CONICET) Güemes 3450-3000 Santa Fe, Argentina*

Received 20 August 2002; received in revised form 24 September 2002; accepted 27 November 2002

## Abstract

The role of the non-gelling polysaccharide, propyleneglycol alginate (PGA), on the dynamics of gelation and gel properties of  $\beta$ -lactoglobulin ( $\beta$ -lg) under conditions where the protein alone does not gel (6%) was analyzed. To this end, the kinetics of gelation, aggregation and denaturation of  $\beta$ -lg in the mixed systems (pH 7) were studied at different temperatures (64–88 °C). The presence of PGA increased thermal stability of  $\beta$ -lg. The rate of  $\beta$ -lg denaturation was decreased and the onset and peak denaturation temperatures increased by 2.2–2.4 °C. PGA promoted the formation of larger aggregates that continued to grow in time. An average aggregate diameter of approximately 300 nm is reached at the gel point in the mixed  $\beta$ -lg+PGA systems, irrespective of the heating temperature. Comparing the activation energies for the aggregation (193 kJ/mol), denaturation (422 kJ/mol) and formation of the primary gel structure ( $1/t_{\text{gel}}$ ) (256 kJ/mol) processes in the mixed protein–polysaccharide system, it can be concluded that the rate determining step in the formation of the primary gel structure would be the aggregation of protein.  $E_a$  values for the processes after the gel point (solid phase gelation) suggest a diffusion limited process because of the high viscosity of the solid gelling matrix. The characteristics of the mixed  $\beta$ -lg + PGA gels in terms of rheological and textural parameters, water loss and microstructure were studied as a function of heating temperature and time. The extent of aggregation and the type of interactions involved, prior to denaturation seem to be very important in determining the gel structure and its properties.

© 2003 Elsevier B.V. All rights reserved.

**Keywords:** Thermodynamic incompatibility; Kinetics; Gelation; Aggregation; Denaturation

## 1. Introduction

Both proteins and polysaccharides contribute to the structural and textural properties of foods through their aggregation and gelation behavior.

The development of novel gelled products from proteins and polysaccharides and their control

\* Corresponding author. Fax: +54-11-4576-3366.

E-mail address: [apilosof@di.fcen.uba.ar](mailto:apilosof@di.fcen.uba.ar) (A.M.R. Pilosof).

<sup>1</sup> Consejo Nacional de Investigaciones Científicas y Técnicas de la República Argentina.

needs a better understanding of gelation mechanisms and physical properties of mixed gels.

Use of mixed proteins and polysaccharides is gaining importance because of their synergistic interactions that offer the possibility for controlling or improving gel properties. The phenomenon—known as thermodynamic incompatibility—is commonly exhibited by semi-dilute or concentrated mixed solutions of protein + polysaccharide and is the main cause of synergistic effects.

Incompatibility mainly occurs at pHs higher than the protein isoelectric pH and/or at high ionic strengths [1]. Phase separation of protein–polysaccharides occurs above a critical concentration. At lower concentrations, the protein and the polysaccharide co-exist in a single phase containing the biopolymers in domains in which they mutually exclude one another, a situation that increases the thermodynamic activity of each one, and results in specific changes in functional properties [2–4]. Gelation kinetics, capacity and mechanical properties of protein gels are greatly affected by the presence of incompatible polysaccharides. A consequence of polymer incompatibility is the lowering of the critical concentration for gelation of the components and the acceleration of the aggregation [5,6].

$\beta$ -lactoglobulin ( $\beta$ -lg), the most abundant protein in whey, is its primary gelling agent and dominates the thermal behavior of the total whey protein system [7].

Therefore its thermal denaturation has been extensively studied [8–10] as well as its aggregation and gelation behavior [11,12].

Upon heating,  $\beta$ -lg undergoes complex changes. Raising the temperature, the dimer structure, predominant in aqueous solutions at pH 5.5–7 dissociates to the monomers [13]. Above 60 °C the monomer is partially unfolded and non-polar groups, and the buried thiol group, are exposed [14]. Subsequent protein aggregation can take place depending mainly on protein concentration and pH [15]. At neutral pH thiol/disulfide exchange reactions, leading to the formation of disulfide bonds, are mainly involved. At pH 6, the contribution of thiol groups in the formation of aggregates is lower and large aggregates formed at this pH are mainly physical aggregates [11].

At pH 7, a protein–polysaccharide repulsive interaction may be expected since  $\beta$ -lg and most polysaccharides are negatively charged. The presence of a repulsive protein–polysaccharide interaction leads to a rise of chemical potential, or in other words of the thermodynamic activity of protein in solution [16]. Non-gelling gums (propylene glycol alginate (PGA), xanthan gum,  $\lambda$ -carrageenan added at 0.5–6 wt.%  $\beta$ -lg dispersion (where the protein alone does not gel) promoted the sol–gel transition of  $\beta$ -lg [17]. The time needed for the formation of the gel at pH 7 decreased in the order PGA > xanthan >  $\lambda$ -carrageenan. This would reveal different abilities of gums to increase the ‘effective concentration’ of  $\beta$ -lg, or in other words, the degree of incompatibility.

SEM photomicrographs of mixed  $\beta$ -lg/gum gels revealed particulate microstructures, except for  $\beta$ -lg/PGA gel at pH 7 [17].  $\beta$ -lg/PGA gels consisting of a continuous and dense structure without apparent pores, showed the highest values for texture parameters.

The aim of present work was to study the role of the non-gelling polysaccharide, PGA, on the dynamics of gelation and gel properties of  $\beta$ -lg under conditions where the protein alone does not gel (6%). To this end, the kinetics of gelation, aggregation and denaturation of  $\beta$ -lg in the mixed systems (pH 7) were studied at different temperatures (64–88 °C).

## 2. Experimental

### 2.1. Sample preparation

$\beta$ -lg samples containing the genetic variants A and B were kindly supplied by Besnier-Bridel (France) and PGA was purchased from Sanofi Bio Industries. The  $\beta$ -lg content in the dried powder was about 95% of dry matter. The powder samples were dissolved separately in double filtered (0.2 nm Millipore) distilled water and pH was adjusted with 1 N NaOH. The  $\beta$ -lg/PGA mixed systems were prepared by mixing the  $\beta$ -lg and PGA solutions at 1:1 ratio.

## 2.2. Aggregation of $\beta$ -lg

The aggregation process was carried out in a heat-quench treatment: glass tubes containing about 6 ml of the solutions were heated at several temperatures between 68 and 84 °C in a dry bath. At several consecutive times 1 ml of the solution was taken and placed in 1.5-ml Eppendorf tubes and the reaction was quenched by placing the tubes in ice water. The samples were diluted in distilled water before light scattering measurements.

## 2.3. Light scattering

Dynamic light scattering experiments were carried out in a Dynamic Laser Light Scattering Photometer (Brookhaven Instruments) provided with a He–Ne laser (632.8 nm) and a Digital Correlator Model BI-2000 AT. Measurements were carried out at a fixed scattering angle of 90°. The quartz cuvette containing the sample was thermostatted at 25 °C by means of an external thermostatic bath. The average scattered intensity ( $I_s$ ), related to the number, size and rate of formation of  $\beta$ -lg aggregates and the apparent mean hydrodynamic diameter  $d$  [18], assuming spherical aggregates, were evaluated. Both  $d$  and  $I_s$  were obtained from the measured discrete autocorrelation function of the scattered light intensity. The mean diameter was estimated through the cumulants method [19]. The average scattered light intensity was calculated from the baseline of the autocorrelation function. The commercial software provided by Brookhaven Instruments was employed to achieve these results.

## 2.4. Differential scanning calorimetry

A Mettler TA 4000 DSC was used to study the thermal transition of  $\beta$ -lg pure or in mixed systems. Measurements were made using 40  $\mu$ l volume aluminium pans containing about 20 mg of solutions, with an empty pan as reference.

The mixed solutions were heated at 10 °C/min from 5 to 95 °C. The onset denaturation temperature ( $T_{\text{onset}}$ ) was determined by the intersection with the baseline of the extrapolated leading edge

of the heating curve. The peak temperature ( $T_p$ ) indicating the apparent denaturation temperature was determined from the maximum heat flow. The total calorimetric apparent enthalpy change ( $\Delta H_T$ ) was calculated from the peak area using a straight baseline between the onset and final temperatures of the thermal transition. All calorimetric parameters reported are means of two replicates.

The activation energy ( $E_a$ ) was determined by the method of Borchardt and Daniels [20] using the equation:

$$(k_d)_T = A \exp\left(\frac{-E_a}{RT}\right) = \left(\frac{\Delta H_T}{c_0}\right)^{n-1} \frac{dH/dt(T)}{(\Delta H_{\text{rem}}(T))^n} \quad (1)$$

where  $(k_d)_T$  is the rate constant,  $E_a$  the activation energy,  $A$  the pre-exponential factor,  $n$  the order of the reaction,  $c_0$  the initial reactant concentration,  $\Delta H_T$  the total enthalpy,  $dH/dt$  the heat flux and  $\Delta H_{\text{rem}}$  the residual enthalpy from  $T$ .

$\ln(k_d)$  for various  $n$  values was plotted against  $1/T$  and the order of the reaction was determined by the value of  $n$  that gave the best linear fit.

## 2.5. Tilting test

The time for sol–gel transition ( $t_{\text{til}}$ ) was determined by a tilting test. Solutions of 6%  $\beta$ -lg/0.5% PGA (1 ml) were heated for various lengths of time at constant temperature, held at 5 °C overnight and then tilted. The  $t_{\text{til}}$ , was reached when there was no deformation of the meniscus upon tilting.

## 2.6. Small strain measurements

Dynamic oscillation measurements were performed in a Phar Physica controlled stress Rheometer (MCR 300). Pure  $\beta$ -lg or mixed  $\beta$ -lg+PGA solutions initially at 20 °C were poured onto the bottom plate of a parallel plate measuring system, gap 1 mm. The temperature of the bottom plate was controlled with a Peltier system (Viscotherm VT2, Phar Physica), and liquid paraffin was applied to the exposed surfaces of the sample to prevent evaporation. The frequency was 1 Hz and

the strain was kept at 0.01%. The samples were heated from 20 °C to the final temperature at a rate of 25 °C/min and then kept at constant temperature during a sufficient time to allow  $G'$  to increase by a factor of 100 approximately. The temperature at which the storage and loss modulus ( $G'$  and  $G''$ ) crossed over was taken as the gel point ( $t_{\text{gel}}$ ). The frequency dependence of  $G'$ ,  $G''$  and  $\tan \delta$  was measured at 20 °C with a constant strain of 1% at a frequency range of 0.01–10 Hz.

### 2.7. Gel formation

Mixed gels were formed by heating the solutions contained in glass tubes (19-mm diameter) in a dry bath. The heat treatment was performed at constant temperatures between 72 and 88 °C, with a heating time of 120 min. The systems heated at 72 and 76 °C, were also treated for longer periods to obtain self-supporting gels (7 and 10 h, respectively).

### 2.8. Gel texture

Texture parameters were evaluated by a compression test performed on cylindrical specimens of the gels (19 mm diameter  $\times$  15 mm high), equilibrated at room temperature ( $25 \pm 1$  °C). A texture profile analysis was performed with a Stable Micro Systems TA-XT2i Texture Analyser using a cylindrical probe (P/36R 36 mm diameter). Samples were compressed to 30% of their original heights at a compression rate of 0.5 mm/s. The average of two replicates was reported.

### 2.9. Water loss

Water loss of gels was determined by a net-test [40]. The moisture loss (WL) was calculated as: (weight of juice released/weight of gel)  $\times$  100. The WL values presented are means of at least two replicates.

### 2.10. Transmission electron microscopy

Small pieces were cut out of the gels prepared for texture measurements and fixed for 12 h at 4 °C in 2% (w/w) glutaraldehyde (in a 2% w/w

sodium phosphate buffer, pH 7.2). Samples were rinsed with buffer and post fixed in 1% osmium tetroxide in buffer for 2 h at 4 °C; then rinsed in buffer for 90 min and dehydrated in grade ethanol series (50–100%). The samples were placed in propylene oxide and then embedded in Epon 812 (72 h, 60 °C). Sections (40–60 nm) were stained with uranyl acetate followed by Reynold's lead citrate, and examined by a Jeol 1200 EXII Electron Microscope at 85 kV.

## 3. Results and discussion

### 3.1. Gelation kinetics

Storage modulus ( $G'$ ) and loss modulus ( $G''$ ) were recorded to reflect the structure development during heating  $\beta$ -lg+PGA at different temperatures. Fig. 1 shows the time evolution of  $G'$  and  $G''$  at 76 °C. The temperature evolution is also depicted in the figure. In all samples, gel points determined as the  $G'$ ,  $G''$  crossover, occurred during the holding period at constant temperature. At the protein concentration used in the present work (6%), no gelation ( $G'$ ,  $G''$  crossover) was observed for pure  $\beta$ -lg solutions. The gelation times ( $t_{\text{gel}}$ ) of  $\beta$ -lg+PGA systems, determined at the gel point, decreased from 160 to 13 min when the temperature was increased from 72 to 84 °C (Table 1). At the gel point, where a critical matrix mass is formed, the primary spatial structure of the

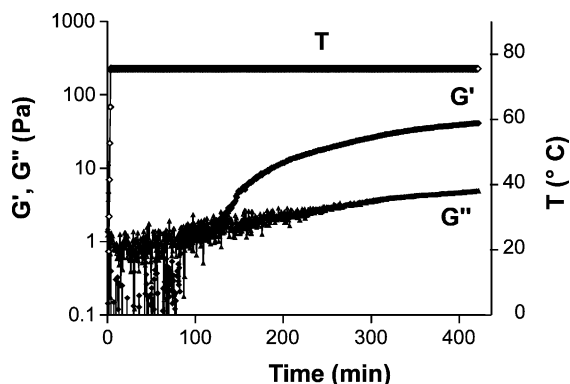


Fig. 1.  $G'$  and  $G''$  evolution during the heat-induced gelation of  $\beta$ -lg+PGA solutions at 76 °C. The temperature profile is also depicted.

Table 1

Gelation times from small strain measurements ( $t_{\text{gel}}$ ) and tilting test ( $t_{\text{til}}$ ) and corresponding denatured protein as a function of heating temperature

$T$ ( $^{\circ}\text{C}$ )	$t_{\text{gel}}$ (min)	Denatured protein (%) at $t_{\text{gel}}$	$t_{\text{til}}$ (min)	Denatured protein (%) at $t_{\text{til}}$
72	160	3.4	–	–
76	120	13	200	20.3
80	38	20.5	80	37.7
84	13	32.7	50	77.4

gel is fixed. The rate of formation of this primary gel structure may be evaluated as  $1/t_{\text{gel}}$ . By plotting  $\ln(1/t_{\text{gel}})$  versus  $1/T$  the Arrhenius plot in Fig. 2 is obtained. From the slope of this plot ( $R^2 = 99.02\%$ ) the calculated activation energy involved in the formation of the primary gel structure was  $256 \pm 18$  kJ/mol.

For all temperatures, both  $G'$  and  $G''$  developed similarly. However, the predominantly elastic gels exhibited final  $G'$  values 10 times greater in magnitude than  $G''$  values. As a result, only  $G'$  values are discussed.  $G'$  values greatly increased during the holding time and finally started to level off. However a plateau value was not reached within the experimental heating times (150–600 min). The protein that is incorporated in the gel network after the gel point gives rise to a ‘thickening’ of the strands in the gel [21]. Consequently, gel rigidity increased after the gel point by a factor of approximately 100. The heating times required to increase gel rigidity by a factor of approximately 100 were 10–40 times greater than

the gelling times. This phenomenon indicates that the sticking together of large aggregates is a slow process.

As the heating rate during the gelling process was very high (from  $20$   $^{\circ}\text{C}$  to the final temperature of  $72$ – $84$   $^{\circ}\text{C}$  at  $25$   $^{\circ}\text{C}/\text{min}$ ) the gelation can be considered to occur at constant temperature. The time evolution of  $G'$  after the gel point was fitted by the following equation [22]:

$$G' = G'_{\infty}(1 - \exp(-k_G t)) \quad (2)$$

where  $G'_{\infty}$  is the plateau value of  $G'$  after a long time and  $k_G$  refers to the rate constant of gel structure development. Fitting Eq. (2) to the  $G'$ -time data, high regression coefficients were obtained ( $R^2 = 98.8$ – $99.9\%$ ). The temperature dependence of the rate of structure development was small as indicated by the low activation energy ( $78 \pm 3$  kJ/mol) obtained from the Arrhenius plot of  $k_G$  in Fig. 2. Therefore, it can be concluded that temperature mainly affects the rate of formation of the primary gel structure, its further development being less affected by heating temperature.

The sequence of events during the course of thermally induced protein gelation can be separated into those that occur in the fluid and solid phases [23]. The dividing line between fluid and solid phase reactions is the gel point ( $t_{\text{gel}}$ ), where the liquid is transformed to a solid. The primary gel structure as well its further development (after  $t_{\text{gel}}$ ) occur as a result of denaturation/aggregation reactions. After the gel point, when entering the solid phase of gelation, aggregation could be diffusion limited because of the high viscosity of the gel matrix.

The gelling times obtained by the tilting test were higher than those obtained from small strain

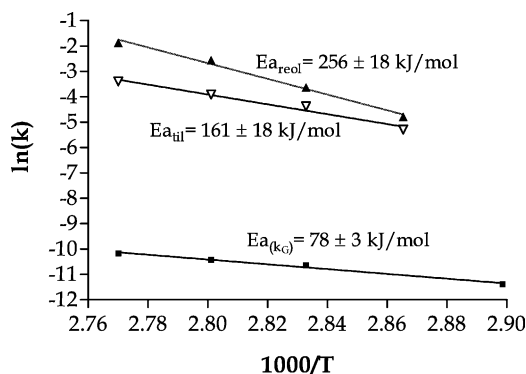


Fig. 2. Arrhenius plots for the rates of gelation obtained from small strain measurements ( $1/t_{\text{gel}}$ ), tilting test ( $1/t_{\text{til}}$ ) and  $G'$  development after the gel point ( $k_G$ ).

measurements (Table 1), because a more developed gel structure is needed to resist the deformation imposed by tilting. At those times ( $t_{\text{til}}$ ) the  $G'$  modulus had already increased by a factor 20–50 depending on the heating temperature. The activation energy obtained by plotting  $\ln(1/t_{\text{til}})$  versus  $1/T$  (Fig. 2) showed an intermediate value ( $161 \pm 18$  kJ/mol) between the activation energies obtained for  $1/t_{\text{gel}}$  and  $k_G$ . This seems reasonable because  $t_{\text{til}}$  embraces both steps, the formation of the primary gel structure and its further development.

### 3.2. Denaturation kinetics

In Table 2, the onset and peak temperatures ( $T_{\text{onset}}$  and  $T_p$ ) and the total enthalpy changes ( $\Delta H_T$ ) determined from DSC thermograms, are given for pure  $\beta$ -lg and  $\beta$ -lg+PGA solutions. The parameters obtained for pure  $\beta$ -lg solutions are in agreement with those reported by several authors that have studied the thermal stability of  $\beta$ -lg under similar conditions of pH and heating rate [12]. In the presence of PGA the thermal stability of  $\beta$ -lg was increased, this effect being reflected by the increase in  $T_{\text{onset}}$ ,  $T_p$  and total enthalpy changes.

In the presence of PGA an increase of 2.2–2.5 °C was observed in the onset and peak temperatures of  $\beta$ -lg denaturation. The apparent enthalpy changes correspond to dimer dissociation and denaturation processes (endothermic) which are superimposed on an aggregation process (exothermic) during the time scale of DSC measurements [24].

At or about neutral pH and at 25 °C,  $\beta$ -lg in solution exists in dynamic equilibrium between its dimeric form in which the monomers are non-covalently linked and the monomeric form [25].

Table 2

Onset temperature ( $T_{\text{onset}}$ ), peak temperature ( $T_p$ ) and total enthalpy changes ( $\Delta H_T$ ) of pure  $\beta$ -lg (6 wt.%) and  $\beta$ -lg (6 wt.%) + PGA (0.5 wt.%)

	$T_{\text{onset}}$ (°C)	$T_p$ (°C)	$\Delta H_T$ (kJ/mol)
$\beta$ -lg	$75.4 \pm 0.2$	$84.6 \pm 0.4$	$3.85 \pm 0.38$
$\beta$ -lg+PGA	$77.9 \pm 0.5$	$86.8 \pm 0.4$	$5.99 \pm 0.54$

Mean values  $\pm$  standard deviation.

Various authors have suggested that dimer dissociation is a necessary step in the heat denaturation process [14,26] and this reaction is favored during heating at neutral pH [11]. A molecular interpretation of the contributions of the different reaction steps involved on heating  $\beta$ -lg was obtained by isothermal calorimetry [11]. The dissociation reaction contributes much to the relatively large endothermic heat flow at the early stage of reaction, at low  $\beta$ -lg concentrations. Increases in temperature at pH 7 cause the unfolding of the monomer with disruption of non-covalent bonds and exposure of the thiol and hydrophobic groups, which were previously buried. The thiol group in the modified monomer can induce exothermic thiol/disulphide exchange reactions leading to the formation of covalent aggregates [7,11]. Physical aggregation will involve no, or only a very small, exothermic heat effect [11], leading to increased apparent enthalpy changes.

The kinetic parameters determined by Borchardt and Daniel's method from the calorimetric curves showed that a reaction order of two gave the best Arrhenius plots from the onset of denaturation up to the peak temperature ( $R^2 = 99.7\%$ ). This value coincides with the reaction order reported by Liu et al. at pH 8.0 [12]. Fig. 3 shows the Arrhenius plots for pure  $\beta$ -lg and  $\beta$ -lg+PGA. The obtained  $E_a$  for the pure  $\beta$ -lg agreed with the values reported by Liu et al. for similar pH and protein concentration [12]. The analysis and comparison of kinetic data is not simple because of the occurrence of aggregation. The

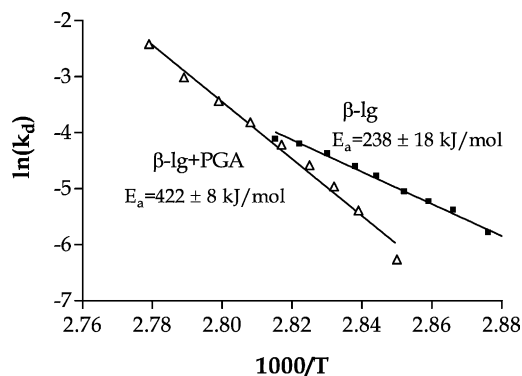


Fig. 3. Arrhenius plots for the rates of denaturation ( $k_d$ ) of pure  $\beta$ -lg and  $\beta$ -lg+PGA solution.



activation energy values for  $\beta$ -lg denaturation increase with protein concentration and this increase is more pronounced at low heating rates [9]. Under these conditions aggregation plays an important role.  $E_a$  strongly increased in the presence of PGA ( $422 \pm 8$  kJ/mol) as shown in Fig. 3, revealing a concentration-like effect, due to the presence of a repulsive protein–polysaccharide interaction that would rise the thermodynamic activity of protein in solution [27].

The presence of PGA decreased the rate of  $\beta$ -lg denaturation (Fig. 3) in accordance with the increased thermal stability of  $\beta$ -lg as revealed by the calorimetric parameters (Table 2).

Percent protein denatured at the corresponding gel point times from small strain measurements ( $t_{gel}$ ) and tilting test ( $t_{til}$ ) could be estimated from the rate constants for  $\beta$ -lg denaturation at 72, 76, 80 and 84 °C (Table 1). At the gel point the amount of protein denatured ranged within 3.4–32.7% for temperatures within 72 and 84 °C. The amount of protein denatured up to the time where a non-deformable gel forms upon tilting ( $t_{til}$ ), ranged from 20.3% for 72 °C to 77.4% for 84 °C.

### 3.3. Aggregation kinetics

Dynamic light scattering has been used for studying the heat-induced aggregation of  $\beta$ -lg over a wide range of medium conditions [15,18,28]. This technique gives quantitative and qualitative information about the aggregates formed during heating, as well as on the rate of particle formation.

In Fig. 4 the apparent hydrodynamic diameters of aggregates formed during heating at different temperatures are shown as functions of heating time. Although 6% pure  $\beta$ -lg solutions did not gel, the protein aggregated upon heating. In the pure  $\beta$ -lg solution the aggregates formed were small (40–60 nm), even for the higher heating temperatures, and after a short time reached a constant value. The plateau value is not due to reaction of all native protein, but because particles of a constant weight-averaged mass are formed [29]. The mean diameter of these aggregates at 76 °C was approximately 50 nm (Fig. 4). The presence of PGA promoted the formation of larger aggregates

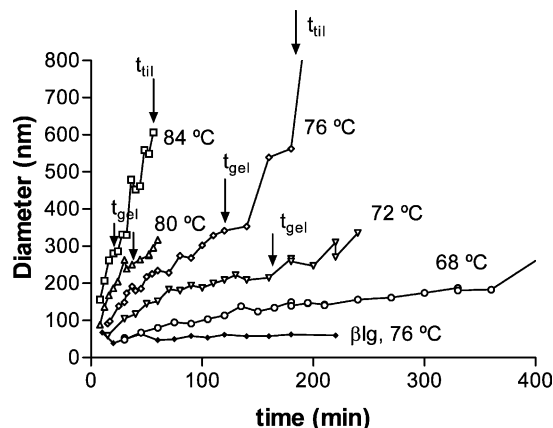


Fig. 4. Apparent diameter of  $\beta$ -lg aggregates formed in the presence of PGA at different heating temperatures. Includes the diameter of aggregates formed at 76 °C in pure  $\beta$ -lg solution.

that continued to grow in time. A similar behavior has been reported for  $\beta$ -lg in the presence of other polysaccharides. Xanthan increased diameters of  $\beta$ -lg aggregates [17,30];  $\kappa$ -carrageenan accelerated the aggregation of small  $\beta$ -lg particles to larger fractal constituents [5];  $\lambda$ -carrageenan (0.5%) promoted the formation of very big particles (8  $\mu$ m) in  $\beta$ -lg gels (6%) [17]. Recently, it was reported that increased concentration of amylopectin accelerated the particle aggregation of  $\beta$ -lg because of phase separation between the protein and the polysaccharide rich phases [31].

The diameters of protein aggregates increased with heating temperature, but a change in the temperature dependence of the particles' size was observed at around 80 °C that is close to the onset temperature of protein denaturation (77.9 °C). Above this temperature a faster increase of the aggregates' diameter with temperature may be observed (Fig. 5). The arrows ( $t_{gel}$ ) in Fig. 4 indicate the gel point as determined by small strain measurements (Table 1). It can be seen that an average aggregate diameter of approximately 300 nm is reached at the gel point in the mixed  $\beta$ -lg + PGA systems, irrespective of the heating temperature. Two phases are distinguished in the aggregation process, being the onset time of the secondary aggregation the gel point, in which the particles size shows a sharp increase with time (see aggregation at 76 °C). Curves at 76 and 84 °C show that

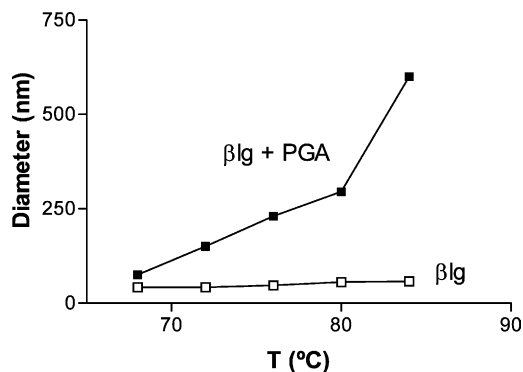


Fig. 5. Apparent diameter of aggregates formed after heating 50 min at different temperatures the pure  $\beta$ -Ig solution and the  $\beta$ -Ig+PGA solution.

the particle sizes at the tilting gelation time (200 and 50 min respectively) are similar, being approximately 800–600 nm. At this time the amount of denatured protein is 20.3 and 77.4%, respectively (Table 1). This suggests that the formation of the particles at the higher temperature should mainly involve exchange reactions between thiol groups exposed upon protein unfolding. However, the lower amount of denatured protein at 76 °C suggests that the formation of aggregates would take place by a combination of chemical and physical aggregation.

In Fig. 6 the scattering intensity,  $I_s$ , is shown as a function of time for different temperatures. The scattered intensity of a particle dispersion in first-

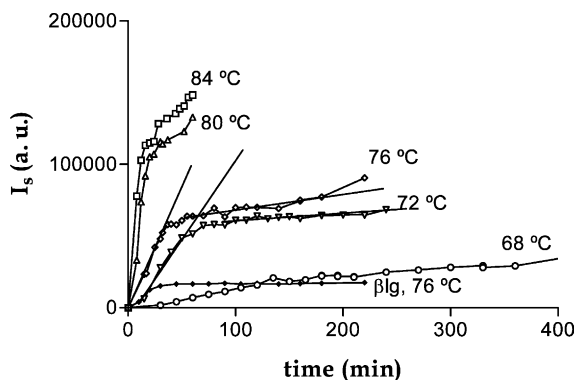


Fig. 6. Scattered intensity ( $I_s$ ) of  $\beta$ -Ig aggregates formed in the presence of PGA at different heating temperatures. Includes the scattered intensity of aggregates formed at 76 °C in pure  $\beta$ -Ig solution. The slopes of the first and the second aggregation phase are indicated for 72 and 76 °C.

order approximation is proportional to the particle weight concentration and the molar mass of the particles [32]. The behavior of pure  $\beta$ -Ig solution (76 °C) was similar to that reported by Hoffman et al. for protein concentrations within 1.5 and 10 and temperatures within 61 and 70 °C [29]. There is an initial fast increase in  $I_s$  with time; furthermore a maximum in  $I_s$  versus time is seen, which is proportional to the square of the polymer particle size [29], that remained constant in the pure  $\beta$ -Ig solution. The scattering intensity at 76 °C was strongly increased in the presence of PGA. The  $I_s$  seemed to reach a plateau value at approximately 100 min, but after the gel point was reached (120 min), the scattered intensity grew again with heating time. At 80–84 °C, because of the rapid evolution of  $I_s$  with time, two consecutive phases with different slopes were apparent, the initial rate of  $I_s$  increase being higher than the second. The second increase in  $I_s$  after the gel point, seems to be correlated to the secondary aggregation at the gel point, in which the particle size shows a sharp increase with time (Fig. 4).

The initial increase of the scattered intensity  $(dI_s/dt)_0$ , taken from the initial slope of the curves describes the rate of protein aggregation during the formation of the primary gel structure in  $\beta$ -Ig+PGA systems (before the gel point). In the case of the pure  $\beta$ -Ig solutions, it also describes the aggregation rate but the gel is not formed. In Fig. 7, the Arrhenius plots for the initial aggregation

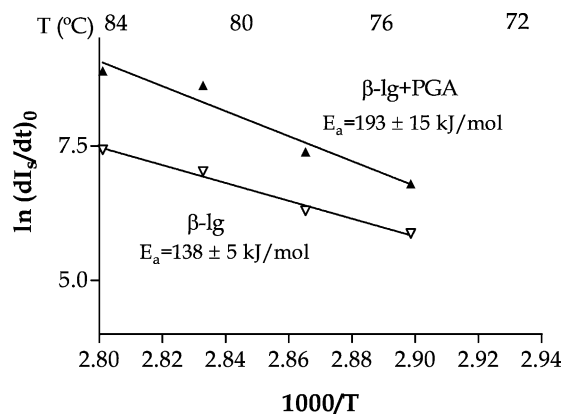


Fig. 7. Arrhenius plots for the rates of initial aggregation of pure  $\beta$ -Ig and  $\beta$ -Ig+PGA solution.



rates for pure  $\beta$ -lg and  $\beta$ -Ig+PGA systems are shown. It can be seen that the main effect of PGA was to strongly increase the rate of  $\beta$ -lg aggregation. The activation energy of  $\beta$ -lg aggregation was increased in the presence of PGA from  $138 \pm 5$  kJ/mol to  $193 \pm 15$  kJ/mol.

The second increase of the scattered intensity ( $dI_a/dt$ ) after the gel point, taken from the slopes of the second phase in Fig. 6, describes the rate of protein aggregation when the gel structure starts to develop during the solid phase of gelation. The activation energy for this secondary aggregation ( $204 \pm 12$  kJ/mol) was similar to that corresponding to the initial aggregation.

### 3.4. Analysis of the kinetic data

The heat-induced gelation of  $\beta$ -lg can be described by a simplified mechanism consisting of two consecutive steps: a denaturation step followed by several aggregation reactions involving chemical and physical bonds. The rate of chemical processes involving several reactions is generally limited by one of the steps. The activation energy of the overall process mainly coincides with the activation energy of the limiting reaction rate step.

Comparing the  $E_a$  values for the aggregation (193 kJ/mol), denaturation (422 kJ/mol) and formation of the primary gel structure ( $1/t_{gel}$ ) (256 kJ/mol) processes in the mixed protein–polysaccharide system, it can be concluded that the rate determining step in the formation of the primary gel structure would be the aggregation of protein. At neutral pH and low ionic strength the aggregation reactions are limiting the gelation rate of pure  $\beta$ -lg [32,33]. Even without comparing the activation energy values, the same conclusion may be reached considering the following: if the denaturation step would have been the rate limiting step, the addition of the polysaccharide that delays protein denaturation, would result in a decrease of the gelation rate. This is opposite to what was experimentally found as  $\beta$ -lg alone at 6% concentration did not gel and in the presence of the polysaccharide gelled.

In spite of the delaying effect that PGA has on the rate of  $\beta$ -lg denaturation (it increases the thermal stability of the protein), its great influence

in promoting protein aggregation (the rate determining step) results in the formation of aggregated particles large enough (300 nm) to form the primary gel structure, that further develops with heating time until the final gel structure is reached.

Similarly, by comparing the  $E_a$  values for the processes after the gel point (solid phase gelation) it appears that the value corresponding to the gel structure development (78 kJ/mol) is well below the  $E_a$  values for the denaturation/aggregation reactions (422 and 204 kJ/mol respectively) involved in the gel formation. This result would suggest a diffusion limited process because of the high viscosity of the solid gelling matrix. Therefore, mass transfer processes would limit the rate of gelation instead of the chemical reactions involved (i.e. denaturation/aggregation).

### 3.5. Gel properties

The characteristics of the mixed  $\beta$ -Ig+PGA gels in terms of rheological and textural parameters, water loss and microstructure were studied as a function of heating temperature and time.

The heating time at each temperature (Table 3) was sufficient to allow  $G'$  to increase by a factor approximately 100 during the heating period.

Fig. 8 shows the frequency dependence of  $G'$  at 20 °C for  $\beta$ -Ig+PGA gels formed at temperatures between 72 and 88 °C. As described by Stading and Hermansson [34], the frequency dependence can provide information about gel structure. The degree of frequency dependence can be expressed by the constant  $n$ :

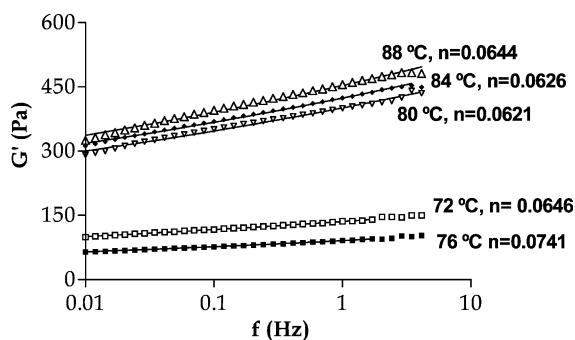
$$\log G' = n \log f + K \quad (3)$$

where  $G'$  is the storage modulus,  $f$  is the oscillation frequency and  $K$  is a constant. For all the mixed systems, similar  $n$  values were obtained, which are indicated in Fig. 8. The  $n$  value was regarded as an indication of the viscoelastic nature of the gels [35]  $n$  is zero for purely elastic gels and becomes higher with increasing relative contribution from the viscous component (less elastic). The  $n$  values obtained indicate the predominantly elastic nature of the gels. It can be seen that above 76 °C, close to the onset of protein denaturation,  $G'$  values showed a dramatic increase. According to rubber

Table 3

Viscoelastic properties of  $\beta$ -Ig (6 wt.%) + PGA (0.5 wt.%) gels heated at different temperatures and heating times

$T$ ( $^{\circ}\text{C}$ )	Heating time (min)	$G'$ (Pa) (1 Hz)	$G''$ (Pa) (1 Hz)	$\tan \delta$ (1 Hz)
72	600	136	15.5	0.114
76	420	91	12.9	0.141
80	240	400	35.1	0.0878
84	180	424	41.1	0.0969
88	120	455	43.9	0.0964

Fig. 8. Frequency sweeps of  $\beta$ -Ig+PGA gels formed at different temperatures.

elasticity theory,  $G'$  should be large at higher temperatures [36,37]. The  $\beta$ -Ig+PGA gels exhibited such a relationship. An increase in  $G'$  during heating and after cooling is indicative of covalent and hydrophobic interactions contributing to matrix rigidity [37]. The same behavior was shown by other rheological parameters in Table 3. Above  $76^{\circ}\text{C}$   $G''$  strongly increased and  $\tan \delta$  decreased.  $\tan \delta$  is considered to represent the relative viscoelasticity within the network [38]. According to this, the gels formed at higher temperatures were more viscoelastic, because they exhibited lower values of  $\tan \delta$  after the heat treatment.

The visual appearances of  $\beta$ -Ig+PGA gels heated during 120 min at different temperatures are shown in Fig. 9. Gels formed at  $72$  or  $76^{\circ}\text{C}$  were not self supporting but those formed at  $84$  and  $86^{\circ}\text{C}$  looked as strong gels. However, gels heated at  $72$  or  $76^{\circ}\text{C}$  could also be structured to give self-supporting gels, by heating for an extended time (10 and 7 h, respectively), as also shown in Fig. 9.

Texture properties of the gels heated during 120 min at different temperatures are shown in Fig. 10. Hardness showed a great increase with heating temperature. The increase of heating time strongly modified the characteristics of the gels formed at  $76^{\circ}\text{C}$ , showing higher values of hardness than the gels formed at  $80^{\circ}\text{C}$  when heated for long time periods. Water loss from gels was low for all the samples ( $< 5\%$ ) irrespective of the heating temperature.

Elasticity and cohesiveness were almost constant for the gels formed at temperatures higher than  $80^{\circ}\text{C}$  (heating time 120 min). The characteristics of the non self-supporting gels formed at  $76^{\circ}\text{C}$  are responsible for the marked decrease in these parameters. However, with longer heating times (7–10 h), the gels formed at lower temperatures were much more elastic and cohesive than those formed at  $80$ – $88^{\circ}\text{C}$ .

The results indicate a great change in the properties of the gels above the onset denaturation temperature of the protein. This behavior may be attributed to a large increase of protein denaturation above  $76^{\circ}\text{C}$ , that could contribute to covalent crosslinks within the gel network (i. e. disulfide bonds).

At temperatures  $72$ – $76^{\circ}\text{C}$ , the denaturation rate is relatively low and the formation of physical aggregates would predominate as shown above (Table 1). The subsequent gel matrix formation through covalent bonding of those aggregates would also occur slowly, allowing the formation of a fine-stranded and homogeneous structures. As shown in Fig. 9 the gels formed at lower temperatures (7–10 h) were translucent, and exhibited a great water holding capacity, high elasticity and cohesiveness. At temperatures above  $80^{\circ}\text{C}$ , the

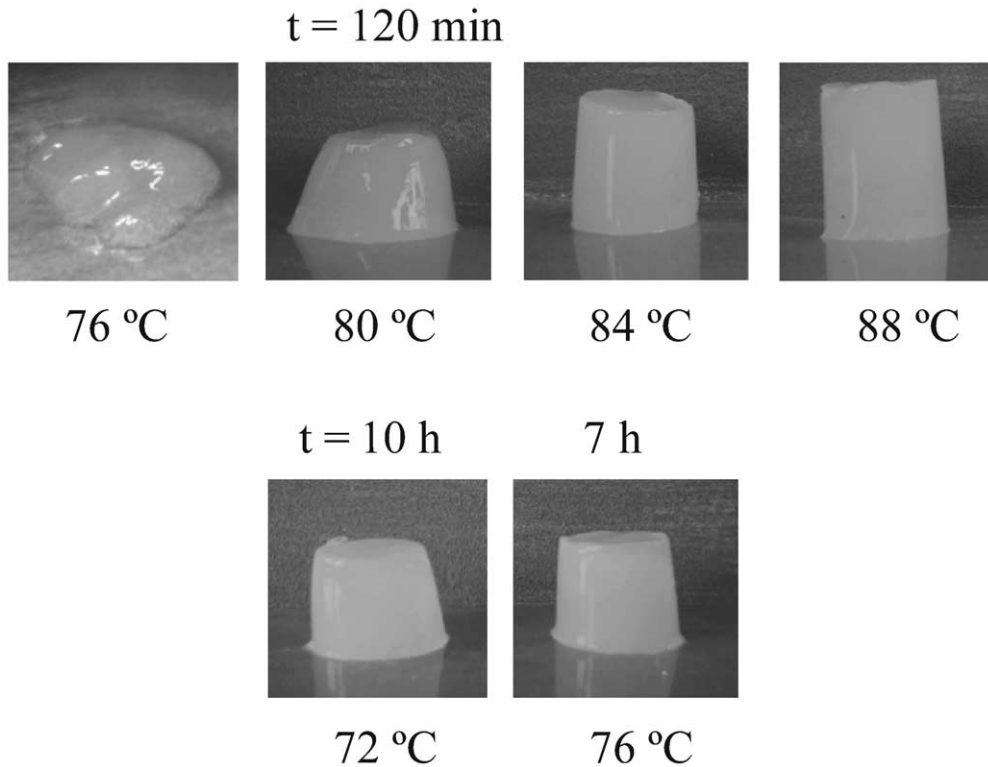


Fig. 9. Visual appearance of  $\beta$ -Ig+PGA gels.

gels were more opaque and stronger, due to the higher level of denatured  $\beta$ -Ig involved in the gel structure at temperatures above the onset of denaturation (Table 1).

Fig. 11 shows the microstructures of the gels formed at temperatures between 80 and 88 °C. Although all these gels were fine stranded, this being their microstructure observed by TEM techniques, they showed notable differences. At 88 °C the structure was homogeneous but denser than at 80 °C. Stading et al. [39] studied the effect of heating rates on the characteristics of fine-stranded  $\beta$ -Ig gels formed at pH 7.5. They found that fast heating rates led to the formation of homogeneous networks composed of thick strands. TEM images of those gels presented a denser and more homogeneous structure. The effect of the heating rate could be associated

with the changes observed in the present work at higher heating temperatures. In the same studies, Stading et al. observed that viscoelastic parameters ( $G'$ , frequency dependence) correlated well with microstructure of the different fine-stranded gels [39]. In our work, the viscoelastic properties also appear to be related to the composition of strands. Gels with thicker strands at 88 °C had higher  $G'$  and hardness.

However the higher elasticity of gels formed at 72–76 °C (7–10 h) could be related to more flexible strands and a low storage modulus and hardness. A similar behavior was previously reported for  $\beta$ -Ig+PGA gels of variable composition and total solids [17]. The elasticity would be influenced by the nature of the bonds involved in the formation of the aggregates that form the primary gel matrix, which, in the case of gels

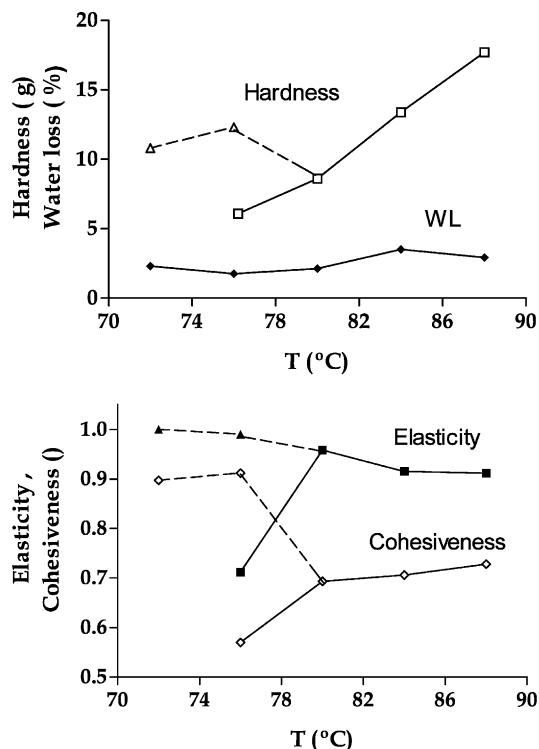


Fig. 10. Gel properties of  $\beta$ -Ig+PGA gels. WL, water loss. The dotted lines indicate gels heated at 72 and 76 °C for 10 and 7 h, respectively. The other points correspond to gels heated 120 min.

formed at low temperatures, involved mainly physical aggregation, due to the low extent of protein denaturation prior to the gel point.

#### 4. Conclusions

The non-gelling polysaccharide, PGA, affects both the denaturation and aggregation processes involved in the heat-induced gelation of  $\beta$ -Ig. This behavior can be ascribed to a limited thermodynamic compatibility between the biopolymers at neutral pH, that increases the thermodynamic activity of the protein.

PGA strongly promotes the aggregation of  $\beta$ -Ig, the rate determining step in gelation, so that aggregates large enough may form the primary gel structure, that further develops over time.

Temperature and heating time have an effect prior to and after the gel point, and alter gel microstructure and functional properties. The extent of aggregation and the type of interactions involved, prior to the gel point seem to be very important in determining the gel structure and its properties.

#### Acknowledgements

The authors acknowledge the financial support from Universidad de Buenos Aires, Universidad Nacional del Litoral, Consejo Nacional de Investigaciones Científicas y Técnicas y Agencia Nacional de Promoción Científica y Tecnológica de la República Argentina.

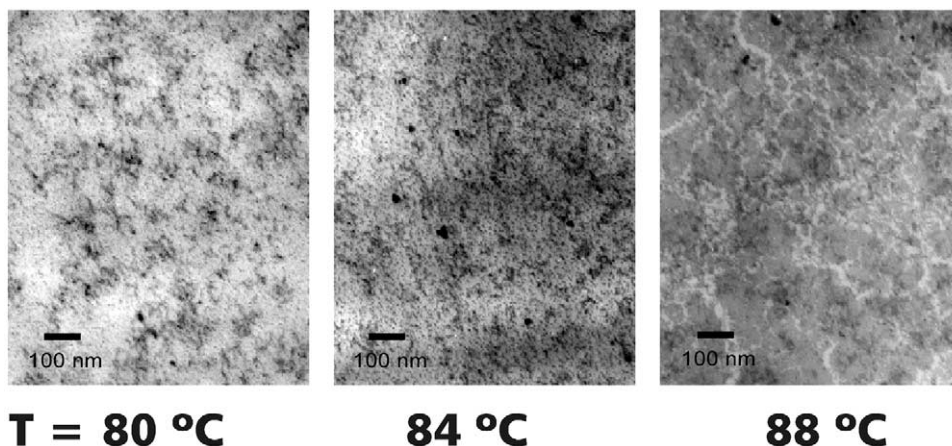


Fig. 11. TEM images of  $\beta$ -Ig+PGA gels formed at different temperatures (120 min).

## References

- [1] V.Y. Grinberg, V.B. Tolstoguzov, *Food Hydrocoll.* 11 (1997) 145.
- [2] D.J. Carp, G.B. Bartholomai, P. Relkin, A.M.R. Pilosof, *Colloid Surf. B* 21 (2001) 163.
- [3] V.E. Sánchez, G.B. Bartholomai, A.M.R. Pilosof, *Lebensm.-Wiss. u.-Technol.* 28 (1995) 380.
- [4] V. Tolstoguzov, in: S. Damodaran, A. Paraf (Eds.), *Food Proteins and Their Applications*, Marcel Dekker, New York, 1997.
- [5] I. Capron, T. Nicolai, D. Durand, *Food Hydrocoll.* 13 (1999) 1.
- [6] M.M. Ould Eleya, S.L. Turgeon, *Food Hydrocoll.* 14 (2000) 29.
- [7] P. Relkin, *Crit. Rev. Food Sci. Nutr.* 36 (1996) 565.
- [8] M. Donovan, D.M. Mulvihill, *Irish J. Food Sci. Technol.* 11 (1987) 87.
- [9] M.A. Hoffmann, P. Van Mil, C.G. De Kruif, in: E. Dickinson, D. Lorient (Eds.), *Food Macromolecules and Colloids*, The Royal Society of Chemistry, UK, 1995.
- [10] P. Relkin, *Thermochim. Acta* 246 (1994) 371.
- [11] M.A. Hoffmann, P.J. Van Mil, *J. Agric. Food Chem.* 47 (1999) 1898.
- [12] T.X. Liu, P. Relkin, B. Launay, *Thermochim. Acta* 246 (1994) 387.
- [13] H.A. Mc Kenzie, W.H. Sawyer, *Nature* 214 (1967) 1101.
- [14] S. Lametti, B. De Gregori, G. Vecchio, F. Bonomi, *Eur. J. Biochem.* 237 (1996) 106.
- [15] M. Verheul, S. Roefs, K. De Kruif, *J. Agric. Food Chem.* 46 (1998) 896.
- [16] V. Tolstoguzov, *Food Hydrocoll.* 11 (1997) 159.
- [17] R. Baeza, A.M.R. Pilosof, in: E. Dickinson, R. Miller (Eds.), *Food Colloids 2000: Fundamentals of Formulation*, The Royal Society of Chemistry, UK, 2001.
- [18] M.A. Hoffmann, S. Roefs, M. Verheul, P. Van Mil, K. De Kruif, *J. Dairy Res.* 63 (1996) 423.
- [19] D. Koppel, *J. Chem. Phys.* 57 (1972) 4814.
- [20] H.J. Borchardt, S.F. Daniels, *J. Am. Chem. Soc.* 79 (1957) 41.
- [21] M. Verheul, *Aggregation and gelation of whey proteins*, Ph.D. Thesis, Universiteit Twente, Enschede, 1998.
- [22] K. Nishinari, M. Watase, M. Rinaudo, M. Milas, *Food Hydrocoll.* 10 (1996) 277.
- [23] E. Foegeding, E. Bowland, C. Hardin, *Food Hydrocoll.* 9 (1995) 237.
- [24] P. Relkin, B. Launay, T.-X. Liu, *Thermochim. Acta* 308 (1998) 69.
- [25] H.A. Mc Kenzie, in: H.A. Mc Kenzie (Ed.), *Milk Proteins: Chemistry and Molecular Biology*, Academic Press, New York, 1971.
- [26] S. Cairoli, S. Lametti, F. Bonomi, *J. Protein Chem.* 13 (1994) 347.
- [27] G.E. Pavlovskaya, M. Semenova, E.N. Thzapkina, V.B. Tolstoguzov, *Food Hydrocoll.* 7 (1993) 1.
- [28] S. Roefs, K. DeKruif, A model for the denaturation and aggregation of  $\beta$ -lactoglobulin, *Eur. J. Biochem.* 226 (1994) 883.
- [29] M. Hoffman, S. Roefs, M. Verheul, P. Van Mil, K. De Kruif, *J. Dairy Res.* 63 (1996) 423.
- [30] D.V. Zasyarkin, E. Dumay, J.C. Cheftel, *Food Hydrocoll.* 10 (1996) 203.
- [31] C. Olson, M. Langton, A.M. Hermansson, *Food Hydrocoll.* 16 (2002) 477.
- [32] M. Verheul, S. Roefs, DeKruif, *J. Agric. Food Chem.* 46 (1998) 896.
- [33] S.M. Taylor, P.J. Fryer, *Food Hydrocoll.* 8 (1994) 45.
- [34] M. Stading, A.-M. Hermansson, *Food Hydrocoll.* 4 (1990) 121.
- [35] S. Ikeda, E.A. Foegeding, *Food Hydrocoll.* 13 (1999) 245.
- [36] J.D. Ferry, *Viscoelastic Properties of Polymers*, Wiley, New York, 1975.
- [37] E. Bowland, E. Foegeding, D. Hamann, *Food Hydrocoll.* 9 (1995) 57.
- [38] J.M. Aguilera, Y.L. Xiong, J.E. Kinsella, *Food Res. Int.* 26 (1993) 11.
- [39] M. Stading, M. Langton, A.-M. Hermansson, *Food Hydrocoll.* 6 (1992) 455.
- [40] A.M. Hermansson, M. Lucisanp, *J. Food Sci.* 47 (1982) 1955.